Abnormal neurotransmission in mice lacking synaptic vesicle protein 2A (SV2A)

Kelly M. Crowder*†, Jane M. Gunther*†, Theresa A. Jones†‡, Brian D. Hale*, Hai Zhuan Zhang*, Michael R. Peterson§, Richard H. Scheller§, Charles Chavkin*, and Sandra M. Bajjalieh*¶

Departments of *Pharmacology and ‡Psychology, University of Washington, Seattle, WA 98195; and §Department of Molecular and Cellular Physiology and Howard Hughes Medical Institute, Stanford University, Stanford, CA 94305

Communicated by William A. Catterall, University of Washington School of Medicine, Seattle, WA, October 21, 1999 (received for review September 13, 1999)

Synaptic vesicle protein 2 (SV2) is a membrane glycoprotein common to all synaptic and endocrine vesicles. Unlike many proteins involved in synaptic exocytosis, SV2 has no homolog in yeast, indicating that it performs a function unique to secretion in higher eukaryotes. Although the structure and protein interactions of SV2 suggest multiple possible functions, its role in synaptic events remains unknown. To explore the function of SV2 in an *in vivo* context, we generated mice that do not express the primary SV2 isoform, SV2A, by using targeted gene disruption. Animals homozygous for the SV2A gene disruption appear normal at birth. However, they fail to grow, experience severe seizures, and die within 3 weeks, suggesting multiple neural and endocrine deficits. Electrophysiological studies of spontaneous inhibitory neurotransmission in the CA3 region of the hippocampus revealed that loss of SV2A leads to a reduction in action potential-dependent γ-aminobutyric acid (GABA)ergic neurotransmission. In contrast, action potential-independent neurotransmission was normal. Analyses of synapse ultrastructure suggest that altered neurotransmission is not caused by changes in synapse density or morphology. These findings demonstrate that SV2A is an essential protein and implicate it in the control of exocytosis.

The release of neurotransmitters is mediated by a secretory cycle that shares many features with general membrane trafficking. Work from several disciplines is beginning to identify a sequence of protein–protein and protein–lipid interactions that mediate the formation, targeting, and fusion of transport vesicles (1). However, neural secretion has several unique features, including the mechanism of vesicle filling, the tight coupling of vesicle exocytosis to the influx of calcium, and the strict localization of vesicle fusion to special ''active'' zones. These features are likely to be mediated by proteins specific to neurons and cells that display regulated secretion.

Synaptic vesicle protein 2 (SV2) was one of the first proteins to be localized to synaptic vesicles (2). Three isoforms have been identified, referred to as SV2A, SV2B, and SV2C (3–6). The absence of SV2 homologs in yeast suggests that it is not a component of the basic membrane trafficking mechanism and, therefore, may mediate a process unique to regulated secretion. The structure and protein interactions of SV2 suggest multiple possible functions, which include acting as a transporter (3–5), providing a matrix for neurotransmitter concentration and release (7), acting as a receptor for extracellular matrix proteins (8), and regulating the action of other synaptic proteins (9). To explore the function(s) of SV2 in an *in vivo* context, we used the technique of targeted gene disruption to produce animals that do not express SV2A. Analyses of these animals were guided by previous studies of SV2 isoform expression (10). In this paper, we report that SV2A is essential for survival and for normal nervous system functioning. Electrophysiological and morphological studies of synapse function and structure suggest that loss of SV2A leads to a reduction in action potential-dependent γ-aminobutyric acid (GABA)ergic neurotransmission and that this decrease is not the result of changes in synapse number or structure.

Methods

Generation of SV2A-Minus Mice. A portion of the SV2A gene was isolated from a mouse 129SV genomic library (Stratagene) by screening with a probe encoding bases −400 to +212 of the rat SV2A cDNA (3). A fragment of ≈12.5 kb was isolated that contained the exon encoding the translation start site through most of the first transmembrane domain of the SV2A cDNA. Mouse SV2A sequence was approximately 95% identical to rat in this region. The location of the exon in the genomic fragment was identified by restriction enzyme mapping and Southern analysis. A targeting construct was generated in pBlueScript in which the exon and surrounding DNA were replaced with a gene encoding neomycin resistance as illustrated in Fig. 1. DNA encoding thymidine kinase was placed at the end of the short arm of the targeting construct to allow for negative selection of homologous recombination by using the antiviral agent Gancyclovir (Syntex, Palo Alto, CA). Embryonic stem cells, a gift from Rejean Idzerda and G. Stanley McKnight (Univ. of Washington), were transfected with linearized targeting construct by electroporation. Cells were placed under selection in G418 (GIBCO/BRL) and Gancyclovir. Resistant colonies were screened for homologous recombination by Southern analysis of *Hin*dIII-digested genomic DNA by using the probe depicted in Fig. 1. Four cell lines carrying the SV2A disruption were injected into C57BL/6 blastocysts and implanted into pseudopregnant females. One of ten chimeric males produced offspring heterozygous for the SV2A gene disruption. These offspring were bred with each other to produce animals homozygous for the mutation. Wild-type offspring of heterozygotes were used to establish a colony of genetically matched control animals. All animals used in these studies were genotyped by Southern analysis of DNA isolated from tail clippings.

Analyses of Protein Expression. Protein expression was determined by immunoblot analysis of 1% Triton X-100 extracts or postnuclear supernatants of whole brain obtained from littermate pups of heterozygote crosses. Equal amounts of protein from wild-type, heterozygous, and homozygous littermates were separated by SDS/PAGE and transferred to nitrocellulose. Proteins were stained with Ponceau Red to verify equivalent loading between lanes. Blots were probed for the indicated protein. Antibody binding was detected by chemiluminescence.

Light Microscopic Analyses. Gross brain morphology was assessed in 10-μm coronal sections from age-matched pups. Mice were

Abbreviations: SV2, synaptic vesicle protein 2; P*n*, postnatal day *n*; GABA, γ-aminobutyric acid; IPSCs, inhibitory postsynaptic currents; mIPSCs, miniature IPSCs; sIPSCs, spontaneous IPSCs; CNS, central nervous system; APV, 2-amino-5-phosphonovaleric acid; CNQX, 6-cyano-7-nitroquinoxaline-2,3-dione.

†K.M.C., J.M.G., and T.A.J. contributed equally to this work.

¶To whom reprint requests should be addressed at: Department of Pharmacology, University of Washington, Box 357280, Seattle, WA 98195. E-mail: bajjalie@u.washington.edu.

The publication costs of this article were defrayed in part by page charge payment. This article must therefore be hereby marked "*advertisement*" in accordance with 18 U.S.C. §1734 solely to indicate this fact.

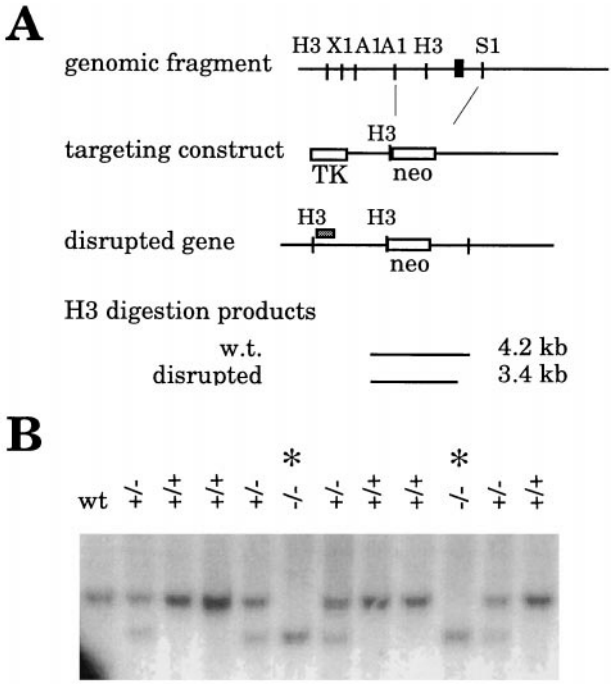

Fig. 1. Targeted disruption of the SV2A gene. (*A*) Strategy for generating SV2A-minus mice. A portion of the SV2A gene was isolated by screening a mouse 129SV genomic DNA library with a probe corresponding to the 5′-end of the rat SV2A cDNA. The exon containing the translation start site is depicted as a black box. A targeting construct was generated in which this exon and surrounding DNA were replaced with a gene encoding neomycin resistance. To allow for negative selection, a gene encoding thymidine kinase was placed at the end of the short arm of the construct. Homologous recombination of the construct resulted in a disrupted gene that produced a shorter fragment when digested with the restriction enzyme *Hin*dIII. Cells and animals were genotyped by Southern analysis of *Hin*dIII-digested genomic DNA probed with the DNA fragment depicted as a gray box above the schematic of the disrupted gene.H3, *Hin*dIII; X1, *Xba*I; A1, *Apa*I; S1, *Spe*I; neo, gene encoding neomycin resistance; TK, gene encoding thymidine kinase; w.t., wild type. (*B*) Southern analysis demonstrating disruption of the SV2A gene. Shown is a Southern analysis of genomic DNA isolated from two litters produced by mice heterozygous (+/−) for the SV2A gene disruption. DNA containing the disruption produces a smaller *Hin*dIII-digestion fragment. Genotypes are indicated at the tops of the lanes. Homozygous mutants are marked with an asterisk. wt, wild type.

asphyxiated with CO_2; brains were removed, embedded in Tissue Tek OCT compound (Sakura Finetek, Torrance, CA), and kept at −80°C until sectioning. Sections were fixed in 4% paraformaldehyde, stained with Toluidine blue, dehydrated, and coverslipped.

Electron Microscopic Analyses. Ultrathin (70-nm) sections of the CA3 region of the hippocampus were obtained by using methods similar to those described (11). Synapse density was measured by using the physical dissector method (12) in two sets of five serially positioned electron micrographs (final magnification ×25,875). Axodendritic synapses were identified by the presence of at least three vesicles in the presynaptic bouton and by the presence of a postsynaptic density. Synaptic density was calculated as the number of synapses divided by the sample volume. Synaptic structural measures were made by using series of 4–12 electron micrographs per animal, printed at a final magnification of ×42,750. The profile area of boutons was measured by using the technique of systematic point counting (13). The length of postsynaptic densities was measured by using a grid-intersection method. A transparency with a test line system was placed over the micrograph. Intersections between a test line and the length of synaptic densities directly apposing a presynaptic bouton were counted. The length of postsynaptic densities per synapse (estL/synapse) was estimated by using the formula: estL/synapse = $(2 \cdot I \cdot a/l)$/synapses, where I is the total number of intersections between synaptic densities and test lines, a/l is the area represented by a test line (0.058 $\mu m^2/\mu m$, adjusted for magnification), and "synapses" is the number of synapses included in the sample. Synaptic density thickness was estimated by measuring each density at its widest region. This measurement was converted based on rulers photographed at the same magnification as the tissue. Similarly, synaptic vesicle diameter was approximated by measuring up to 10 vesicles in randomly selected synapses and correcting for magnification. All measures were done with mixed, coded micrographs to control for experimenter bias.

Physiological Analyses. Whole-cell voltage clamp recordings were obtained from CA3 pyramidal neurons in mouse hippocampal slices. Most of the mice were ages postnatal day 9 (P9)–10 (8 of 11 wild type and 6 of 7 knockouts), with the rest being P11–13. Mice were decapitated, and their brains were quickly removed, placed in ice-cold cutting buffer (220 mM sucrose/3 mM KCl/4 mM $MgCl_2$/1.25 mM NaH_2PO_4/26 mM $NaHCO_3$/10 mM D-glucose), and equilibrated with 95% O_2/5% CO_2. Transverse 300-μm slices were cut and immediately placed in a holding chamber with oxygenated artificial cerebrospinal fluid buffer (128 mM NaCl/3 mM KCl/2 mM $CaCl_2$/2 mM $MgCl_2$/1.25 mM NaH_2PO_4/26 mM $NaHCO_3$/10 mM D-glucose). Recording pipettes were filled with an internal recording solution (130 mM CsCl/1 mM EGTA/0.5 mM $CaCl_2$/2 mM $MgCl_2$/2 mM ATP-Mg/10 mM Hepes/1.5 mM QX-314, pH adjusted to 7.2–7.4 with CsOH). The resulting pipet resistance was 4–6 MΩ. Recordings were done at room temperature in a submersion chamber while the cell was held at −70 mV. Infrared-aided Nomarski differential interference contrast video microscopy was used to select a viable pyramidal cell in the CA3 region. Series resistance was monitored continuously throughout the recording. Recordings with series resistance <30 MΩ were analyzed. Variation in series resistance was not compensated and varied, on average, 20%. We observed no effect of series resistance flux on event frequency. All recordings were performed in the presence of 25 μM APV (2-amino-5-phosphonovaleric acid) and 10 μM CNQX (6-cyano-7-nitroquinoxaline-2,3-dione). The recording bath also included 300 nM tetrodotoxin to block presynaptic action potentials in recordings of miniature inhibitory postsynaptic currents (mIPSCs). Both mIPSCs and spontaneous inhibitory postsynaptic currents (sIPSCs) were verified as GABAergic, at the conclusion of 40% of the recordings, by using the GABA-A receptor antagonist, bicuculline methiodide (10 μM; Sigma). In all cases, bicuculline blocked all events. Both sIPSCs and mIPSCs were measured by using an Axopatch 200B amplifier (Axon Instruments, Foster City, CA). Recordings were filtered at 1 kHz (80 dB per decade, 4-pole low-pass Bessel filter) and digitally sampled at 5 kHz (Digidata 1200 and pClamp6; Axon Instruments). Events were analyzed by using MINI ANALYSIS PROGRAM (Synaptosoft, Leonia, NY), which employs a threshold-based event-detection algorithm. Frequencies and amplitudes of sIPSCs and mIPSCs were measured in 2-min epochs, taken at least 4 min after the initiation of recording, by using the software event detector set to identify events above background. mIPSC events were visually inspected to ensure no false mIPSCs were included in data sets. The two-tailed Student's t test was used to assess statistical significance.

Results and Discussion

Targeted Disruption of the SV2A Gene. A portion of the SV2A gene containing the translation start site was isolated as described under *Methods* and used to generate the targeting construct

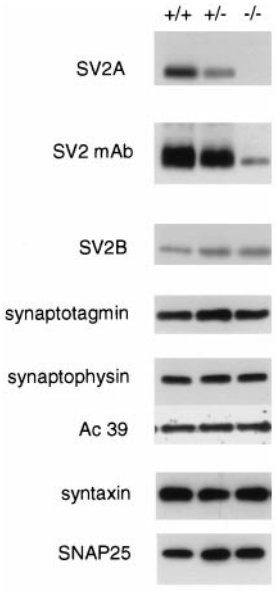

Fig. 2. Disruption of the SV2A gene results in the absence of SV2A protein but does not significantly alter the expression of other synaptic proteins. Shown are immunoblot analyses of brain protein isolated from wild-type (+/+) mice and littermates heterozygous (+/−) and homozygous (−/−) for the SV2A mutation. SV2A expression was detected by using an isoform-specific polyclonal antibody. Mice heterozygous for the mutation express significantly less SV2A than wild-type littermates, and homozygous mutants express nondetectable levels. Western analysis using the anti-SV2 monoclonal antibody, which recognizes an epitope present in all known SV2 isoforms, revealed that SV2A knockouts (−/−) express very little total SV2 protein. This suggests that SV2A is the primary SV2 isoform in mouse brain. This decrease is seen even though the expression of SV2B is increased in these animals. Expression levels were normal for the synaptic proteins synaptotagmin I, synaptophysin, and the 39-kDa accessory subunit of the H^+/ATPase (Ac 39), and for the t-SNAREs syntaxin and SNAP-25.

depicted in Fig. 1. This construct was used to generate mice homozygous for the SV2A gene disruption. SV2A mutants were, on average, 50% 129SVJ and 50% C57BL/6. To control for effects of a mixed genetic background and the possibility of additional mutations that may have occurred in the generation of disrupted embryonic stem cell lines, wild-type animals used in these studies were descendants of the founding chimeric male.

Mice homozygous for the SV2A gene disruption express no SV2A protein as detected by immunoblot (Western) analysis (Fig. 2). Total SV2, detected with a monoclonal antibody that recognizes an epitope present in all known isoforms, was also significantly reduced in the brain of SV2A knockouts. It therefore seems that SV2A is the predominant isoform of SV2 in mouse brain. Both heterozygous and homozygous SV2A mutants expressed higher levels of SV2B than wild types did, suggesting that the expression of these SV2 isoforms is co-regulated. However, this increase did not significantly raise total SV2 levels. Loss of SV2A did not affect the expression of the SV2A-binding protein synaptotagmin I, indicating that synaptotagmin expression and stability are not dependent on SV2A. There was also no effect on the expression of several other synaptic proteins, including synaptophysin (14), the 39-kDa subunit of the H^+/ATPase (15) or the target-localized, soluble *N*-ethylmaleimide-sensitive factor attachment protein receptors (t-SNAREs) syntaxin (16), and SNAP-25 (refs. 17 and 18; Fig. 2).

Northern analyses using a probe to the 3′-end of the rat SV2A cDNA revealed that SV2A mutants do not express a full-length SV2A mRNA (data not shown). Long exposures revealed a truncated message expressed at lower levels than the full-length wild-type mRNA. These results, combined with the Western analyses, suggest that no SV2A protein is produced in the knockouts. However, because all available antibodies are directed against the amino terminus of SV2A, we cannot rule out the possibility that a truncated SV2A protein is expressed.

SV2A Knockouts Appear Normal at Birth but Fail to Grow, Experience Severe Seizures, and Die by the Third Week of Life. Animals homozygous for the SV2A gene disruption constitute approximately one-quarter of live births resulting from the mating of heterozygous mutants. This indicates that SV2A is not required for embryonic development. Indeed, SV2A knockouts are not readily distinguishable from littermates until approximately P7. However, after P7, the growth rate of knockouts falls significantly behind that of both wild types and heterozygotes. By P9, homozygotes are approximately one-half the size of littermates. The fact that heterozygous mutants are of normal size indicates that a single copy of SV2A is sufficient to support growth. SV2A homozygous mutants are no more likely to die as neonates than their littermates, however they die between P12 and P23, with an average life span of 16.5 ± 2.4 days (n = 28). Heterozygous mutants have a slightly higher mortality rate in the second through sixth months versus wild types, but in general are viable, of normal body weight, and fertile.

All SV2A homozygous mutants experience severe motor seizures. The age of onset, P6–P10, parallels the developmental conversion of GABA from an excitatory to an inhibitory neurotransmitter in the central nervous system (CNS) (19, 20). Seizures are generalized in nature, which is indicative of widespread CNS hyperexcitability. Interestingly, heterozygous mutants also experience seizures. We have observed spontaneous seizures during routine cage changes in 24% (47/197) of the SV2A heterozygous mutants, as compared with 2.7% (5/182) of wild types. The seizure phenotype in heterozygotes is interesting in light of their viability and normal size. This suggests that CNS functioning is especially sensitive to SV2A expression levels.

The effects of the SV2A mutation on growth, CNS excitability, and mortality indicate that SV2A is an essential protein and are consistent with defects in multiple neuroendocrine systems. For example, the growth deficit may result from effects of the SV2A mutation on hormone secretion. Likewise, SV2A-knockout animals die at the time when pups become reliant on their own insulin production, suggesting that death could be caused by aberrant energy metabolism. The presence of multiple secretory deficits is also suggested by the observation that the management of seizures with medication does not reverse the growth defect nor prevent death in SV2A knockouts (K.M.C. and S.M.B., unpublished data).

Loss of SV2A Does Not Alter Gross Brain Morphology. The brains of knockouts were smaller than wild types, in proportion with their reduced body size. However, examination of Nissl-stained brain section revealed no major differences in the relative size or morphology of major brain structures, including the hippocampus, cortex, and thalamic structures (Fig. 3). Cerebellar morphology was also normal (data not shown). This indicates that the seizure phenotype of the SV2A mutants is not caused by gross CNS anomalies.

Inhibitory Neurotransmission Is Reduced in the Hippocampus of SV2A Mutants. Previous analyses of SV2-isoform expression in rat revealed that SV2A is expressed in all neurons and is the only known isoform expressed in most GABAergic neurons and in hippocampal dentate granule cells (10), glutamatergic neurons that provide major excitatory input to GABAergic interneurons in the hippocampus (21). These neurons are predicted to be devoid of SV2 in SV2A knockouts and, therefore, to be espe-

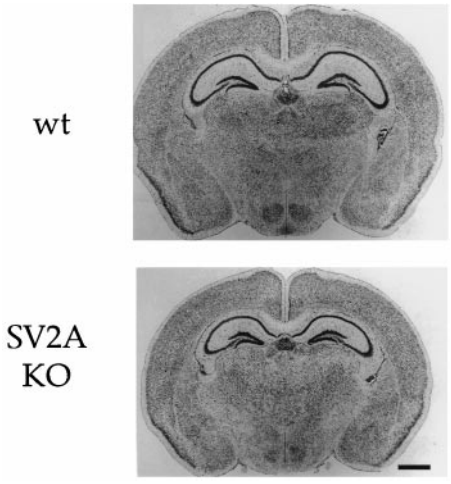

Fig. 3. Gross brain morphology is normal in SV2A-knockout mice. Shown are Nissl-stained coronal sections of brain from P14 wild-type and SV2A-knockout mice. The brains of SV2A-knockout mice are smaller, in proportion with their reduced body size. However, major brain structures, including the cerebral cortex, hippocampus, and thalamus, appear normal. Cerebellar morphology was also normal (data not shown). wt, wild type; KO, knockout.

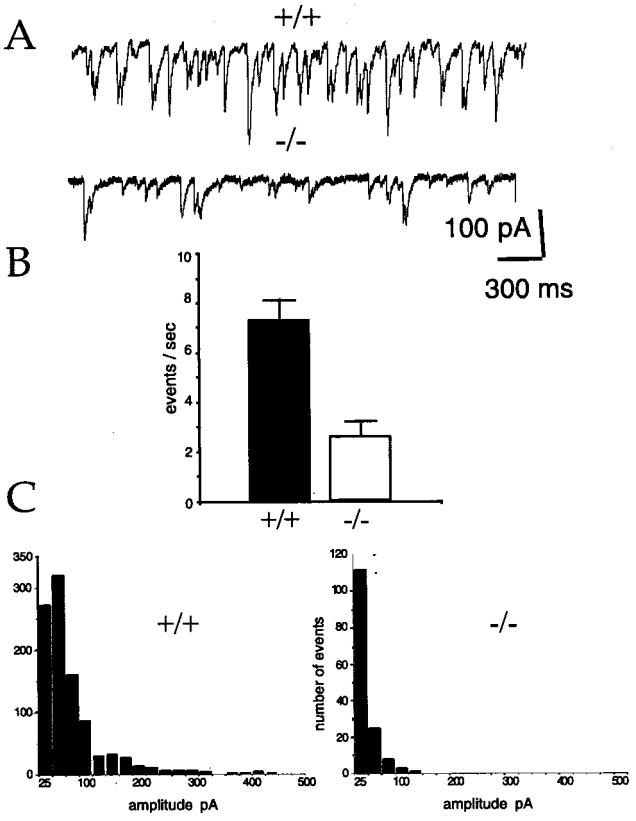

Fig. 4. GABAergic neurotransmission is reduced in the hippocampus of SV2A-knockout animals. sIPSCs were measured in hippocampal CA3 pyramidal neurons. Recordings were made in the presence of the glutamate receptor blockers CNQX and APV. (*A*) Sample traces from wild-type (+/+) and SV2A-knockout (−/−) cells. Shown are 4-sec traces of sIPSCs recorded from representative cells. The downward deflection of the events is the result of outward chloride flux in the cells voltage-clamped at −70 mV. Currents were filtered at 1 kHz and digitized at 5 kHz. There was no digital filtering of the recordings to decrease noise in the traces shown. (*B*) Averaged sIPSC frequencies. Shown are histograms representing average sIPSC frequencies. Each was calculated from 30 2-min epochs. Wild-type values were obtained from six cells from six (+/+) animals. Knockout values were obtained from seven cells from five (−/−) animals. Error bars indicate SEM. Rates were significantly different as determined with the Student's *t* test ($P \ll 0.01$). (*C*) Frequency histograms of sIPSC amplitude. A frequency analysis of event amplitudes binned in 25-pA increments is shown. Data were derived from recordings of six cells from six (+/+) animals and seven cells from four (−/−) animals. For each cell, a single 2-min epoch of representative frequency was selected. All events detected by the detection program were verified by visual inspection. Note that there were many fewer events in (−/−) cells. The average amplitude in (−/−) cells was roughly half that of events in (+/+) cells, 24.85 pA ± 7.8 vs. 51.2 pA ± 6.8 for the knockouts and wild type, respectively ($n = 4$ each).

cially affected. If SV2 is required for normal neurotransmission, its absence in these neurons should result in aberrant inhibitory neurotransmission, which could underlie the seizure phenotype of the SV2A mutants. To test this possibility, we examined GABAergic neurotransmission in a hippocampal slice preparation. Previous studies have revealed high levels of endogenous GABAergic neurotransmission in the hippocampus (22), most of which is action potential-dependent (23). This spontaneous GABA release is hypothesized to control hippocampal excitability (22, 24). Whole-cell recordings of sIPSCs in CA3 pyramidal neurons were made in slices obtained from animals aged P9 to P12, with the majority coming from P9–P10 animals to control for seizure-induced changes in the mutants. All recordings were done in the presence of the glutamate receptor blockers CNQX and APV to prevent fast, excitatory neurotransmission. The frequency of sIPSCs was high in wild-type CA3 neurons, displaying an average of 7.3 Hz, a rate that agrees with previous reports of sIPSC rates in rat hippocampus (22). In contrast, sIPSC frequency averaged 2.6 Hz in SV2A knockouts (Fig. 4), less than half of that found in wild-type neurons. sIPSC amplitude was also significantly reduced in SV2A knockouts as compared with wild types, 23.3 ± 7.8 pA (SEM) vs. 51.2 ± 6.8 pA, respectively ($n = 4$). This reduced amplitude is consistent with the decreased frequency of events, the majority of which reflect concomitant transmitter release at multiple sites. The simplest interpretation of these results is that loss of SV2A reduces GABA secretion. However, because these recordings measured naturally occurring activity, we cannot distinguish between direct and indirect effects. For example, decreased GABAergic transmission could also be caused by a decrease in excitatory input to GABAergic neurons via metabotropic glutamate receptors or increased inhibitory input carried by neuropeptides. In either case, it is clear that loss of SV2A results in abnormal inhibitory neurotransmission in the hippocampus, which is likely to contribute to the seizure phenotype.

To determine whether reduced inhibitory neurotransmission in SV2A knockouts reflects alterations in the basic machinery of membrane fusion, we measured the frequency of mIPSCs in CA3 neurons. Recorded in the presence of the sodium channel blocker tetrototoxin, mIPSCs represent action potential-independent transmitter release. A decrease in mIPSC frequency would indicate that SV2 is a component of the basic fusion machinery, whereas an increase would suggest that it acts as a negative regulator of vesicle fusion. In wild-type cells, tetrototoxin reduced the frequency of total spontaneous IPSCs by 90%, resulting in an average frequency of 0.52 Hz and confirming previous reports that most of the spontaneous inhibitory neurotransmission in the hippocampus is action potential-dependent (22, 24). mIPSC frequency was similar in neurons from SV2A-knockout animals, averaging 0.50 Hz (Fig. 5). The lack of a difference in mIPSC frequency suggests that SV2 is not required for vesicle fusion, an interpretation consistent with its absence in yeast. mIPSC amplitude, which reflects the number of postsynaptic receptors (25), was also measured. We observed similar mIPSC amplitudes in wild-type and SV2A-knockout

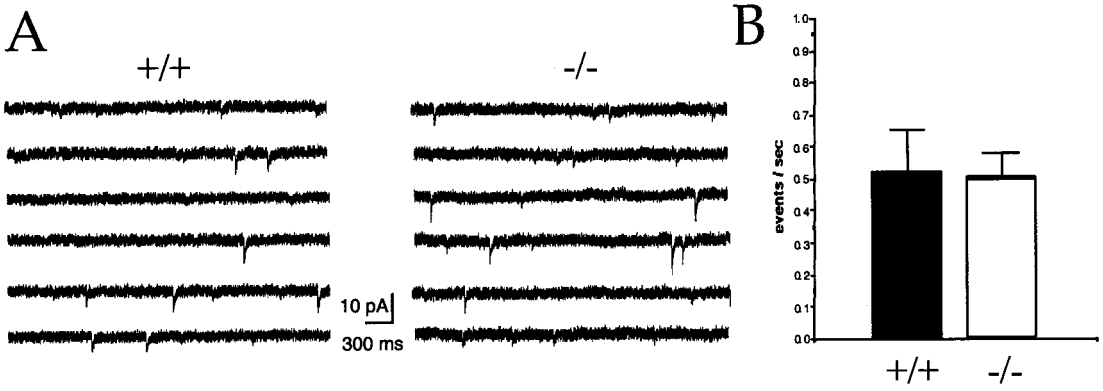

Fig. 5. Action potential-independent neurotransmission is not affected in SV2A-knockout animals. (*A*) Sample traces from wild-type (+/+) and SV2A-knockout (−/−) cells. Shown are representative 23-sec sweeps of mIPSCs from whole-cell voltage clamp recordings of hippocampal CA3 pyramidal cells held at −70 mV. Recordings were made in the presence of the glutamate receptor blockers APV and CNQX and the sodium channel blocker tetrototoxin. (*B*) mIPSC frequencies were similar in cells from wild type and SV2A knockouts. Histograms illustrating the average frequency of mIPSCs recorded from nine (+/+) cells (six animals) and nine (−/−) cells (six animals). Error bars indicate SEM. Rates were not significantly different as determined with the Student's *t* test ($P = 0.79$).

neurons. In fact, amplitudes were slightly larger in SV2A-mutant cells (data not shown). These results suggest that loss of SV2A does not significantly reduce the expression or action of postsynaptic receptors and are consistent with the interpretation that SV2A is not involved in the regulation of quantal size.

Loss of SV2A Does Not Alter Synapse Density or Morphology. The observation that SV2 binds the extracellular matrix protein laminin (8) suggested that it could participate in the formation of synapses or the establishment of active zones. To determine whether the reduced neurotransmission in SV2A knockouts is caused by changes in synapse density and/or morphology, synapses were analyzed at the electron microscopic level. Two areas of the CA3 region of the hippocampus were chosen for examination: the CA3 pyramidal neuron cell-body layer and the proximal region of CA3 apical dendrites. CA3 cell bodies receive inhibitory input from GABAergic interneurons via symmetric synapses (26), whereas proximal dendrites receive mossy fiber input from dentate granule neurons via asymmetric, presumed excitatory synapses (27). These synapses express SV2A primarily or exclusively (10, 28) and, therefore, were predicted to be especially affected by the SV2A gene disruption. Visual inspection of micrographs revealed no differences in the density or morphology of either synapse type (Fig. 6).

Quantitative structural analyses were performed on the more numerous mossy fiber synapses onto proximal dendrites of CA3 pyramidal neurons. As listed in Table 1, synapse density was similar in wild type and SV2A knockouts, indicating that loss of SV2A does not affect the establishment or pruning of these synapses. Synapse morphology was also not significantly altered. We found no difference in the size of synaptic boutons, active zone length, postsynaptic density thickness, or in the clustering of vesicles (measured as the number of vesicles per unit area). It remains possible that SV2A plays a role in the strengthening of synapses and that the effects of the mutation on this function are not apparent in young animals. However, it appears that the observed phenotype of SV2A knockouts is not attributable to aberrant synapse formation or morphology.

We also determined whether the loss of SV2A affected synaptic vesicle formation, stability, or size, by comparing the number of synaptic vesicles and vesicle diameter between wild type and SV2A knockouts. The average number of synaptic vesicles per synapse did not differ (Table 1). Likewise, vesicle diameters were similar and agreed with previously reported measurements (29). This normal vesicle phenotype contrasts with that found in rab3A and synapsins I and II knockouts. The

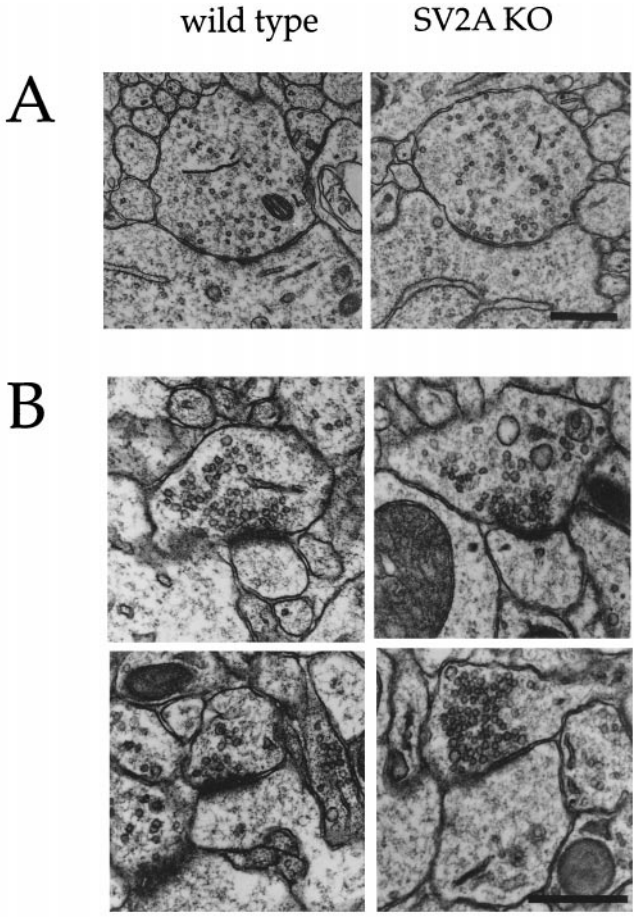

Fig. 6. Synapse morphology is normal in SV2A-knockout mice. (*A*) Shown are representative electron micrographs of symmetric (GABAergic) synapses in the cell-body region of CA3 hippocampal neurons. These synapses are presumed to be GABAergic based on their location, symmetry of active zones, and irregularly shaped vesicles. Qualitative inspection of these synapses suggested no difference in density or morphology between wild type and SV2A knockouts. (*B*) Shown are representative electron micrographs of asymmetric synapses onto proximal dendrites of CA3 hippocampal neurons. Synapses in this region are primarily from dentate granule cells and are largely asymmetric, presumed glutamatergic synapses. Similar morphology was observed in wild type and SV2A knockouts. Quantitative analyses of these synapses are presented in Table 1.

Table 1. Loss of SV2A does not affect synapse number or morphology

	Synapse density, 10^6 synapses/mm^3	Bouton size, area in μm^2	Active zone length, nm	Active zone thickness, nm	Vesicle clustering, vesicles/μm^2	Vesicle number, mean per synapse	Vesicle diameter, nm
Wild type	668	217 ± 147 (86)	370 ± 25 (115)	7.5 ± 22 (115)	2.4 ± 0.5 (86)	19.1 ± 18.2 (114)	30.4 ± 9.4 (155)
SV2A knockout	620	290 ± 208 (88)	412 ± 19 (112)	6.7 ± 26.3 (103)	2.4 ± 0.9 (88)	21.5 ± 17.3 (110)	37.4 ± 9.4 (190)

The proximal dendritic region of CA3 hippocampal neurons, which receives mossy fiber input from dentate granule neurons and which has a predominance of asymmetric, presumed excitatory synapses, was photographed at ×42,750. Photographs were analyzed for the listed features as described under *Methods.* Data were obtained from three wild-type and three SV2A-knockout animals, except for the measure of synapse density, which was obtained from three wild types and two SV2A knockouts. Numbers in parentheses indicate the total number of synapses or vesicles analyzed.

loss of these synaptic vesicle proteins led to a reduction in synaptic vesicle number (30, 31). In a variation of this effect, mutation of the gene encoding the synaptic vesicle protein synaptotagmin, in *Drosophila*, resulted in a decrease in the number of vesicles immediately adjacent to the active zone (32). Although our morphological analyses do not rule out a role for SV2A in the recruitment or maintenance of vesicles at active zones, they do indicate that SV2A is not needed for vesicle formation or stability.

The results presented here demonstrate that SV2A is required for normal neurotransmission. In the absence of SV2A, action potential-dependent GABAergic neurotransmission is aberrant. This effect does not appear to be caused by changes in the number or structure of synapses. Although we cannot rule out the possibility that the decreased neurotransmission is secondary to effects at other synapses, the synapses studied were among the most likely to be affected by the loss of SV2A. An alternate possibility, that the observed phenotype is caused by changes in the ability of GABAergic neurons to produce or sustain action potentials, could result from direct or indirect interactions of SV2 with presynaptic ion channels, a characteristic that has not yet been reported for SV2. The simplest interpretation, however, is that SV2A participates in calcium's triggering of vesicle fusion. A similar function has been ascribed to synaptotagmin (33), a calcium-binding protein that interacts with SV2 (9). *In vitro* binding of SV2 and synaptotagmin is regulated by calcium, suggesting that this complex participates in the control of exocytosis. It is interesting to note that targeted disruption of synaptotagmin I in mice resulted in profoundly reduced evoked transmission without affecting the frequency of action potential-independent exocytosis (33), a phenotype analogous to the SV2A-mutant phenotype. Although the reduced severity of the SV2A phenotype could be caused by the compensatory action of additional, uncharacterized SV2 isoforms, it is also consistent with SV2A acting as a modulator of calcium-stimulated exocytosis rather than as an effector. Such a modulatory role could occur via interaction with synaptotagmin. Further study, of both SV2 mutants and SV2 protein interactions, will more clearly resolve the precise molecular action of SV2 in the synapse.

We thank Drs. Rejean Idzerda and G. Stanley McKnight for supplying ES cells; Kathy Kafer for blastocyst injections; Drs. Philip Schwartzkroin, Jergen Wenzel, and Gregory Terman for helpful discussions; Dr. Roger Janz for sharing information on SV2C expression; and Dr. William Catterall for reviewing the manuscript. Early portions of this work were supported by grants from the Sloan and Whitehall Foundations and an Howard Hughes Medical Institute/University of Washington Pilot Research grant to S.B. This work was funded by the National Institutes of Mental Health Grant R01 MH59842–01. J.G. was supported by Grants DA07278 and NS33898 from the National Institutes of Health.

1. Bajjalieh, S. M. (1999) *Curr. Opin. Neurobiol.* **9,** 321–328.
2. Buckley, K. & Kelly, R. B. (1985) *J. Cell Biol.* **100,** 1284–1294.
3. Bajjalieh, S. M., Peterson, K., Shinghal, R. & Scheller, R. H. (1992) *Science* **257,** 1271–1273.
4. Feany, M. B., Lee, S., Edwards, R. H. & Buckley, K. M. (1992) *Cell* **70,** 861–867.
5. Bajjalieh, S. M., Peterson, K., Linial, M. & Scheller, R. H. (1993) *Proc. Natl. Acad. Sci. USA* **90,** 2150–2154.
6. Janz, R., Hofmann, K. & Sudhof, T. C. (1998) *J. Neurosci.* **15,** 9269–9281.
7. Rahamimoff, R. & Fernandez, J. M. (1997) *Neuron* **18,** 17–27.
8. Son, Y.-J., Scranton, T. W., Sunderland, W. J., Baek, S. J., Miner, J. H., Sanes, J. R. & Carlson, S. S., *J. Biol. Chem*., in press.
9. Schivell, A. E., Batchelor, R. H. & Bajjalieh, S. M. (1996) *J. Biol. Chem.* **271,** 27770–27775.
10. Bajjalieh, S. M., Franz, G., Weimann, J. M., McConnell, S. K. & Scheller R. H. (1994) *J. Neurosci.* **14,** 5223–5235.
11. Jones, T. A. (1999) *J. Comp. Neurol.* **414,** 57–66.
12. Gundersen, H. J. G., Bendtsen, T. F., Korbo, L., Marcussen, N., Moller, A., Nielsen, K., Nyengaard, J. R., Pakkenberg, B., Sorensen, F. B., Vesterby, A., *et al.* (1988) *Acta Pathol. Scand.* **96,** 379–394.
13. Royet, J.-P. (1991) *Prog. Neurobiol.* **37,** 433–474.
14. Wiedenmann, B. (1991) *Acta Oncol.* **30,** 435–440.
15. Forgac, M. (1992) *J. Exp. Biol.* **172,** 155–169.
16. Bennett, M. K., Calakos, N. & Scheller R. H. (1992) *Science* **257,** 255–259.
17. Oyler, G. A., Higgins, G. A., Hart, R. A., Battenberg, E., Billingsley, M., Bloom, F. E. & Wilson, M. C. (1989) *J. Cell Biol.* **109,** 3039–3052.
18. Sollner, T., Whiteheart, S. W., Brunner, M., Erdjument-Bromage, H., Geromanos, S., Tempst, P. & Rothman, J. E. (1993) *Nature (London)* **362,** 318–324.
19. Cherubini, E., Gaiarsa, J. L. & Ben-Ari, Y. (1991) *Trends Neurosci.* **14,** 515–519.
20. Rivera, C., Voipio, J., Payne, J. A., Ruusuvuori, E., Lahtinen, H., Lamsa, K., Pirvola, U., Saarma, M. & Kaila, K. (1999) *Nature (London)* **397,** 251–255.
21. Acsady, L., Kamondi, A., Sik, A., Freund, T. & Buzsaki, G. (1998) *J. Neurosci.* **18,** 3386–3403.
22. Otis, T. S., Staley, K. J. & Mody, I. (1991) *Brain Res.* **545,** 142–150.
23. Otis, T. S. & Mody, I. (1992) *Neuroscience* **49,** 13–32.
24. Alger, B. E. & Nicoll, R. A. (1980) *Brain Res.* **200,** 195–200.
25. Nusser, Z., Cull-Candy, S. & Farrant, M. (1997) *Neuron* **19,** 697–709.
26. Eccles, J. (1964) *The Physiology of Synapses* (Springer, Berlin).
27. Collonnier, M. (1968) *Brain Res.* **9,** 268–287.
28. Janz, R. & Sudhof, T. C. (1999) *Neuroscience*, in press.
29. Bekkers, J. M., Richerson, G. B. & Stevens, C. F. (1990) *Proc. Natl. Acad. Sci. USA* **87,** 5359–5362.
30. Geppert, M., Bolshakov, V. Y., Siegelbaum, S. A., Takei, K., De Camilli, P., Hammer, R. E. & Sudhof, T. C. (1994) *Nature (London)* **369,** 493–497.
31. Rosahl, T. W., Spillane, D., Missler, M., Herz, J., Selig, D. K., Wolff, J. R., Hammer, R. E., Malenka, R. C. & Sudhof, T. C. (1995) *Nature (London)* **375,** 488–493.
32. Reist, N. E., Buchanan, J., Li, J., Buxton, E. M. & Schwarz, T. L. (1998) *J. Neurosci.* **18,** 7662–7673.
33. Geppert, M., Goda, Y., Hammer, R. E., Li, C., Rosahl, T. W., Stevens, C. F. & Sudhof, T. C. (1994) *Cell* **79,** 717–727.